

# Deep Generative Models for Sparse, High-dimensional, and Overdispersed Discrete Data

He Zhao\*

Piyush Rai†

Lan Du\*

Wray Buntine\*

Mingyuan Zhou‡

\*Monash University, Australia

†Indian Institute of Technology, Kanpur, India

‡The University of Texas at Austin, USA

## Abstract

Many applications, such as text modelling, high-throughput sequencing, and recommender systems, require analysing sparse, high-dimensional, and overdispersed discrete (count/binary) data. With the ability of handling high-dimensional and sparse discrete data, models based on probabilistic matrix factorisation and latent factor analysis have enjoyed great success in modeling such data. Of particular interest among these are hierarchical Bayesian count/binary matrix factorisation models and nonlinear latent variable models based on deep neural networks, such as recently proposed variational autoencoders for discrete data. However, unlike the extensive research on sparsity and high-dimensionality, another important phenomenon, overdispersion, which large-scale discrete data exhibit, is relatively less studied. It can be shown that most existing latent factor models do not capture overdispersion in discrete data properly due to their ineffectiveness of modelling self- and cross-excitation (e.g., word burstiness in text), which may lead to inferior modelling performance. In this paper, we provide an in-depth analysis on how self- and cross-excitation are modelled in existing models and propose a novel variational autoencoder framework, which is able to explicitly capture self-excitation and also better model cross-excitation. Our model construction is originally designed for count-valued observations with the negative-binomial data distribution (and an equivalent representation with the Dirichlet-multinomial distribution) and it also extends seamlessly to binary-valued observations via a link function to the Bernoulli distribution. To demonstrate the effectiveness of our framework, we conduct extensive experiments on both large-scale bag-of-words corpora and collaborative filtering datasets,

where the proposed models achieve state-of-the-art results.<sup>1</sup>

## 1 Introduction

Discrete data are ubiquitous in many applications. For example, in text analysis, a collection of documents can be represented as a word-document count matrix with the bag-of-words assumption; in recommender systems, users' shopping history can be represented as a count/binary item-user matrix, with each entry indicating whether or not a user has bought an item (or its purchase count). Such data is often characterised by high-dimensionality and extreme sparseness. In recent years, analysing such data, often represented as massive-sized count/binary matrices, has been widely applied to text analysis, graph analysis, medical studies, etc.

With the ability to handle high-dimensional and sparse matrices, Probabilistic Matrix Factorisation (PMF) Mnih and Salakhutdinov (2008) has been a key method of choice for such problems. PMF assumes data is generated from a suitable probability distribution (i.e., the data distribution), parameterised by low-dimensional latent factors. When it comes to discrete data, Latent Dirichlet Allocation (LDA) Blei et al. (2003) and Poisson Factor Analysis (PFA) Canny (2004); Zhou et al. (2012) are the two representative models that generate the samples using the multinomial and Poisson distributions, respectively. Originally, LDA and PFA can be seen as single-layer models, which have limited modelling expressiveness. Therefore, extensive research has been devoted to extending them with hierarchical Bayesian priors Blei et al.

<sup>1</sup>Code at <https://github.com/ethanhezhao/NBVAE>

(2010); Paisley et al. (2015); Gan et al. (2015b); Zhou et al. (2016). However, increasing model complexity with hierarchical priors can also complicate the inference, and lack of scalability hinders their usefulness in analysing large-scale data.

Recently, deep generative models such as Variational Autoencoders (VAEs) Rezende et al. (2014) have become increasingly popular for modelling real-valued data, such as images. The success of VAEs has motivated machine learning practitioners to adapt VAEs to dealing with discrete data as done in recent works Miao et al. (2016, 2017); Krishnan et al. (2018); Liang et al. (2018). Instead of using the Gaussian distribution as the data distribution for real-valued data, the multinomial distribution has been used for discrete data Miao et al. (2016); Krishnan et al. (2018); Liang et al. (2018). Following Liang et al. (2018), we refer to these VAE-based models as “MultiVAE” (Multi for multinomial)<sup>2</sup>. MultiVAE can be viewed as a deep nonlinear PMF model, where the nonlinearity is introduced by a deep neural networks in the decoder. Compared with conventional hierarchical Bayesian models, MultiVAE increases its modelling capacity without sacrificing the scalability, because of the use of amortized variational inference (AVI) Rezende et al. (2014). This makes MultiVAE a good choice for large-scale discrete data.

However, most existing discrete data models (shallow/deep) do not take into consideration another key property of discrete data, *overdispersion* (i.e., variance larger than the mean), which leads to inferior modelling performance. Large-scale discrete data can usually be highly overdispersed, with the data variability being extremely large. One reason why the models using either Poisson or multinomial as the data distribution encounters the overdispersion problem is that, with only one free parameter, the Poisson distribution does not allow the variance to be adjusted independently from the mean; notably, the multinomial distribution faces the similar issue as it can be seen as a normalisation of a set of Poissons.

By contrast, models with the data distribution Zhou (2018); Gouvert et al. (2018), as the negative-binomial distribution consist of one more parameter to adjust the data variance independently of the mean. The Negative-Binomial Factor Analysis (NBFA) model proposed by Zhou (2018) has shown its potential for modelling overdispersion over the PMF models. Zhou (2018) conducted an in-depth analysis on how NBFA captures overdispersion and showed that overdispersion in large-scale discrete data is due to *self-* and *cross-*

<sup>2</sup>In terms of the generative process (encoder), the models in Miao et al. (2016); Krishnan et al. (2018); Liang et al. (2018) are similar, despite that the inference procedures are different.

*excitation* of the attribute frequencies. To be more concrete, self-citation describes the phenomenon that an attribute is expected to occur more in a sample if it shows up once, while cross-citation describes that the occurrence of an attribute triggers the occurrences of some other related ones. A representative example here is word burstiness Church and Gale (1995); Madsen et al. (2005); Doyle and Elkan (2009); Buntine and Mishra (2014), meaning that if a word is seen in a document, it may excite both itself and related ones. Models with Poisson/multinomial do not distinguish between self- and cross-excitation and usually assume that the attributes of a sample are independently generated. Therefore, even with a complex multi-layer structure, the ultimate modelling capacity of modelling self- and cross-excitation in LDA, PFA, and Multi-VAE is limited. In contrast, as shown in Zhou (2018), negative-binomial in NBFA separates self-excitation from cross-excitation and explicitly models the former, making NBFA achieve better modelling performance than the models with multinomial/Poisson. Although self-excitation is directly modelled in NBFA, cross-excitation has to be implicitly captured by the interactions of the latent factors, which requires powerful modelling capacity. Unfortunately, the single-layer structure of NBFA only allows linear combinations of the latent factors, which limits its capacity of modelling cross-excitation.

On the other hand, besides count-valued data, binary matrices are also prevalent, such as in collaborative filtering. Although multinomial and Poisson are candidate choices of the data distribution for modelling counts, it may not be proper to apply them to binary data, which is a common misspecification in many existing models. This is because multinomial and Poisson may assign more than one count to one position, ignoring the fact that the data are binary. The misspecification could result in inferior modelling performance Zhou (2015).

Motivated by the above issues and desiderata, we present a deep generative model called **Negative-Binomial Variational AutoEncoder (NBVAE** for short), a VAE-based framework generating data with a negative-binomial distribution. It has the following attractive properties: **1)** NBVAE is able to handle overdispersion in discrete data by sufficiently capturing both self- and cross-excitation. Specifically, with negative-binomial as the data distribution, NBVAE captures self-excitation explicitly in a similar way to NBFA. Moreover, unlike the single-layer structure of NBFA, the encoder in NBVAE has a deep structure, which can provide a richer capacity to better model cross-excitation. **2)** The usage of negative-binomial in-

stead of multinomial enables us to develop a link function between the Bernoulli and negative-binomial distributions, which gives us a variant of NBVAE that can handle binary data with superior modelling performance. 3) Compared with conventional Bayesian PMF models, the VAE framework with amortised inference makes NBVAE more scalable in dealing with the large-scale discrete data.

With extensive experiments on both large-scale bag-of-words corpora and collaborative filtering datasets, we demonstrate that the negative-binomial distribution and its binary variant are better choices of VAEs for overdispersed discrete data. Compared with several state-of-the-art baselines (both shallow and deep models), NBVAE achieves significantly better performance in both text analysis and collaborative filtering tasks.

## 2 Model Details

In this section, we discuss the details of our proposed models. We start with an introduction of our proposed NBVAE model for count-valued data, and then give a detailed analysis on how self- and cross-excitation are captured in different models and why NBVAE is capable of better handling self- and cross-excitation. Finally, we describe the variant of NBVAE for binary-valued data.

### 2.1 Negative-Binomial Variational Autoencoder (NBVAE)

Like the standard VAE model, NBVAE consists of two major components: the decoder for the generative process and the encoder for the inference process. Here we focus on the generative process and discuss the inference procedure in Section 3.

Suppose the count-valued data that we are dealing with are stored in a  $V$  by  $N$  count matrix  $\mathbf{Y} \in \mathbb{N}^{V \times N} = [\mathbf{y}_1, \dots, \mathbf{y}_N]$ , where  $\mathbb{N} = \{0, 1, 2, \dots\}$ ,  $V$  and  $N$  are the number of attributes and the number of samples, respectively. To generate the occurrences of the attributes for the  $j^{\text{th}}$  ( $j \in \{1, \dots, N\}$ ) sample,  $\mathbf{y}_j \in \mathbb{N}^V$ , we draw a  $K$  dimensional latent representation  $\mathbf{z}_j \in \mathbb{R}^K$  from its prior, a standard multivariate normal distribution. After that,  $\mathbf{y}_j$  is drawn from a (multivariate) negative-binomial distribution with the parameters  $\mathbf{r}_j \in \mathbb{R}_+^V$  ( $\mathbb{R}_+ = \{x : x \geq 0\}$ ) and  $\mathbf{p}_j \in (0, 1)^V$ . Moreover,  $\mathbf{r}_j$  and  $\mathbf{p}_j$  are obtained by transforming  $\mathbf{z}_j$  from two nonlinear functions,  $f_{\theta^r}(\cdot)$  and  $f_{\theta^p}(\cdot)$ , parameterised by  $\theta^r$  and  $\theta^p$ , respectively. The above generative process of  $p(\mathbf{y}_j | \mathbf{z}_j)$  can be for-

mulated as follows:

$$\mathbf{z}_j \sim \mathcal{N}(\mathbf{0}, \mathbf{I}_K), \quad (1)$$

$$\mathbf{r}_j = \exp(f_{\theta^r}(\mathbf{z}_j)), \quad (2)$$

$$\mathbf{p}_j = 1/(1 + \exp(-f_{\theta^p}(\mathbf{z}_j))), \quad (3)$$

$$\mathbf{y}_j \sim \text{NB}(\mathbf{r}_j, \mathbf{p}_j), \quad (4)$$

where NB stands for a negative-binomial distribution.

Given the model construction, conditioned on the latent representation  $\mathbf{z}_j$ , we can compute the values of  $\mathbf{r}_j$  and  $\mathbf{p}_j$ , and then the likelihood of the sample  $\mathbf{y}_j$  can be written as:

$$p(\mathbf{y}_j | \mathbf{r}_j, \mathbf{p}_j) \propto \prod_v^V \frac{\Gamma(r_{vj} + y_{vj})}{\Gamma(r_{vj})} (p_{vj})^{y_{vj}} (1 - p_{vj})^{r_{vj}} \quad (5)$$

where  $\Gamma(\cdot)$  denotes the gamma function,  $y_{vj}$ ,  $r_{vj}$ , and  $p_{vj}$  are the  $v^{\text{th}}$  ( $v \in \{1, \dots, V\}$ ) element of  $\mathbf{y}_j$ ,  $\mathbf{r}_j$  and  $\mathbf{p}_j$ , respectively.

In the above process,  $\mathbf{p}_j$  is a  $V$  dimensional vector, which is the output of  $f_{\theta^p}(\cdot)$ . Alternatively, if we let the output of  $f_{\theta^p}(\cdot)$  be a single number  $p_j \in (0, 1)$  specific to sample  $j$ , according to Theorem 1 in Zhou (2018) we can derive an alternative representation of NBVAE:

$$\mathbf{z}_j \sim \mathcal{N}(\mathbf{0}, \mathbf{I}_K), \quad (6)$$

$$\mathbf{r}_j = \exp(f_{\theta^r}(\mathbf{z}_j)), \quad (7)$$

$$p_j = 1/(1 + \exp(-f_{\theta^p}(\mathbf{z}_j))), \quad (8)$$

$$y_{\cdot j} \sim \text{NB}(r_{\cdot j}, p_j), \quad (9)$$

$$\mathbf{y}_j \sim \text{DirMulti}(y_{\cdot j}, \mathbf{r}_j), \quad (10)$$

where “DirMulti” stands for the Dirichlet-multinomial distribution,  $y_{\cdot j} = \sum_v y_{vj}$  is the total count, and  $r_{\cdot j} = \sum_v r_{vj}$ .

Accordingly, we refer this representation of NBVAE to as NBVAE<sub>dm</sub> (dm for Dirichlet-multinomial). Note that NBVAE<sub>dm</sub> can also be viewed as a deep, non-linear generalization of models based on Dirichlet-multinomial to capture word burstiness Doyle and Elkan (2009); Buntine and Mishra (2014). However, unlike such models where inference is considerably more difficult, our model admits a much simpler and faster inference procedure as detailed in Sec. 3. Another appealing aspect of NBVAE<sub>dm</sub>, when compared with our original model NBVAE, is that NBVAE<sub>dm</sub> has fewer number of model parameters, and gives faster converge speed, which we will show in the experiments.

### 2.2 How NBVAE Captures Self- and Cross-Excitation

After giving the details of NBVAE above, we now examine how it models self- and cross-excitation in large-scale count data. For easy comparison, we first present

Table 1: Comparison of the data distributions

Model	Data distribution	Parameter
PFA	$\mathbf{y}_j \sim \text{Poisson}(\mathbf{l}_j)$	$\mathbf{l}_j = \Phi \boldsymbol{\theta}_j$
LDA	$\mathbf{y}_j \sim \text{Multi}(\mathbf{y}_j, \mathbf{l}_j)$	$\mathbf{l}_j = \Phi \boldsymbol{\theta}_j / \theta_{.j}$
MultiVAE	$\mathbf{y}_j \sim \text{Multi}(\mathbf{y}_j, \mathbf{l}_j)$	$\mathbf{l}_j = \text{softmax}(f_\theta(\mathbf{z}_j))$
NBFA	$\mathbf{y}_j \sim \text{NB}(\mathbf{l}_j, p_j)$	$\mathbf{l}_j = \Phi \boldsymbol{\theta}_j$
NBVAE	$\mathbf{y}_j \sim \text{NB}(\mathbf{r}_j, p_j)$	$\mathbf{r}_j = \exp(f_{\theta^r}(\mathbf{z}_j))$ $p_j = 1/(1 + \exp(-f_{\theta^p}(\mathbf{z}_j)))$
NBVAE <sub>dm</sub>	$\mathbf{y}_j \sim \text{DirMulti}(\mathbf{y}_j, \mathbf{r}_j)$	$\mathbf{r}_j = \exp(f_{\theta^r}(\mathbf{z}_j))$ $p_j = 1/(1 + \exp(-f_{\theta^p}(\mathbf{z}_j)))$

a unified probabilistic matrix factorisation framework:

$$\mathbf{y}_j \sim \mathcal{D}(\mathbf{l}_j), \quad (11)$$

where  $\mathcal{D}$  denotes a probabilistic measure parameterised by  $\mathbf{l}_j$ .

Next, we reformulate the models related to NBVAE using this framework as follows (also summarised in Table 1):

**PFA Canny (2004); Zhou et al. (2012):** It is obvious that PFA directly fits into this framework, where  $\mathcal{D}$  is the Poisson distribution and  $\mathbf{l}_j = \Phi \boldsymbol{\theta}_j$ . Here  $\Phi \in \mathbb{R}_+^{V \times K} = [\phi_1, \dots, \phi_K]$  is the factor loading matrix and  $\boldsymbol{\Theta} \in \mathbb{R}_+^{K \times N} = [\boldsymbol{\theta}_1, \dots, \boldsymbol{\theta}_N]$  is the factor score matrix. In other words,  $\boldsymbol{\theta}_j$  is the latent representation of sample  $j$  and the  $v^{\text{th}}$  row of  $\Phi$  is the latent representation of attribute  $v$ . Their linear combinations determine the probability of the occurrence of  $v$  in  $j$ .

**LDA Blei et al. (2003):** While originally proposed for bag-of-words of documents, LDA explicitly assigns a topic  $z_j^i$  to the  $i^{\text{th}}$  word in document  $j$ ,  $w_j^i$ ,<sup>3</sup> with the following process:  $z_j^i \sim \text{Cat}(\boldsymbol{\theta}_j / \theta_{.j})$  and  $w_j^i \sim \text{Cat}(\phi_{z_j^i})$ , where  $\theta_{.j} = \sum_k \theta_{kj}$  and ‘‘Cat’’ is the categorical distribution. By collapsing (marginalising out) all the topics, we can derive an equivalent representation of LDA, which is in line with the general framework:  $\mathbf{y}_j \sim \text{Multi}(\mathbf{y}_j, \mathbf{l}_j)$ , where  $\mathbf{l}_j = \Phi \boldsymbol{\theta}_j / \theta_{.j}$  and ‘‘Multi’’ stands for the multinomial distribution.

**MultiVAE Miao et al. (2016); Krishnan et al. (2018); Liang et al. (2018):** MultiVAE generates data from a multinomial distribution, whose parameters are constructed by the decoder:  $\mathbf{y}_j \sim \text{Multi}(\mathbf{y}_j, \mathbf{l}_j)$ , where  $\mathbf{l}_j = \text{softmax}(f_\theta(\mathbf{z}_j))$ .

**NBFA Zhou (2018):** NBFA uses a negative-binomial distribution as the data distribution, the generative process of which can be represented as:  $\mathbf{y}_j \sim \text{NB}(\mathbf{l}_j, p_j)$ , where  $\mathbf{l}_j = \Phi \boldsymbol{\theta}_j$ .

Given that NBVAE and NBVAE<sub>dm</sub> are already in this framework, we can compare them to the above models. Without loss of generality, we consider the scenario of text analysis, where the predictive distribution

<sup>3</sup>Note that we use  $w_j^i \in \{1, \dots, V\}$  to denote the  $i^{\text{th}}$  word in document  $j$ , whereas  $y_{v,j}$  to denote the count of occurrences of word  $v$  and  $y_{v,j} = \sum_i \mathbf{1}(w_j^i = v)$ .

Table 2: Comparisons of the predictive distributions

Model	Predictive distribution	Parameters from posterior
PFA/LDA	$l'_{v,j} \propto \sum_k^K \phi_{vk} \theta_{kj}$	$\Phi, \boldsymbol{\theta}_j \sim p(\Phi, \boldsymbol{\theta}_j   \mathbf{Y}^{-ij})$
MultiVAE	$l'_{v,j} \propto \text{softmax}(f_\theta(\mathbf{z}_j))_v$	$\mathbf{z}_j \sim q(\mathbf{z}_j   \mathbf{Y}^{-ij})$
NBFA	$l'_{v,j} \propto (y_{v,j}^{-i} + \sum_k^K \phi_{vk} \theta_{kj}) p_j$	$\Phi, \boldsymbol{\theta}_j, p_j \sim p(\Phi, \boldsymbol{\theta}_j, p_j   \mathbf{Y}^{-ij})$
NBVAE	$l'_{v,j} \propto \frac{y_{v,j}^{-i} + \exp(f_{\theta^r}(\mathbf{z}_j))_v}{(1 + \exp(-f_{\theta^p}(\mathbf{z}_j)))_v}$	$\mathbf{z}_j \sim q(\mathbf{z}_j   \mathbf{Y}^{-ij})$
NBVAE <sub>dm</sub>	$l'_{v,j} \propto y_{v,j}^{-i} + \exp(f_{\theta^r}(\mathbf{z}_j))_v$	$\mathbf{z}_j \sim q(\mathbf{z}_j   \mathbf{Y}^{-ij})$

of the  $i^{\text{th}}$  word in the  $j^{\text{th}}$  document,  $w_j^i$ , conditioned on the other words,  $\mathbf{Y}^{-ij}$ :

$$\begin{aligned} \mathcal{L} = p(w_j^i = v | \mathbf{Y}^{-ij}) &\propto \int p(w_j^i = v | \mathbf{l}'_j) p(\mathbf{l}'_j | \mathbf{Y}^{-ij}) d\mathbf{l}'_j \\ &= \mathbb{E}_{p(\mathbf{l}'_j | \mathbf{Y}^{-ij})} [p(w_j^i = v | \mathbf{l}'_j)], \end{aligned} \quad (13)$$

where  $p(w_j^i = v | \mathbf{l}'_j)$  is the data likelihood given the model parameters obtained from the posterior,  $p(\mathbf{l}'_j | \mathbf{Y}^{-ij})$ . Note that we use  $\mathbf{l}'_j$  to denote the model parameters obtained from the posterior and leave  $\mathbf{l}_j$  to denote the parameters of the data distribution. Given  $\mathbf{l}'_j$ , we have  $p(w_j^i = v | \mathbf{l}'_j) = l'_{v,j} / l'_{.j}$ .

Now we show the details of how different models obtain the predictive distribution parameters  $l'_{v,j}$  according to their posterior distributions in Table 2, where  $y_{v,j}^{-i}$  denotes the number of  $v$ ’s occurrences in document  $j$  excluding the  $i^{\text{th}}$  word. We have the following remarks of the comparisons shown in Table 2: **1)** In the comparison between PFA, LDA, MultiVAE V.S. NBFA, NBVAE, NBVAE<sub>dm</sub>, it can be seen that the latter three models explicitly capture self-excitation via the term  $y_{v,j}^{-i}$  in the predictive distributions. That is to say, if  $v$  appears more in document  $j$ ,  $y_{v,j}^{-i}$  will be larger, leading to larger probability that  $v$  shows up again. On the other hand, PFA, LDA, and MultiVAE cannot directly capture self-excitation because they predict a word purely based on the interactions of the latent representations and pays less attention to how frequently a word appears in a document. Therefore, no matter how complex the interactions of the latent representations are in those models, their potential of modelling self-excitation is still limited. **2)** For NBVAE and NBFA, self- and cross-excitation are modelled separately in their predictive distributions and self-excitation is explicitly captured by  $y_{v,j}^{-i}$ . Therefore, the interactions of the latent factors are only responsible for cross-excitation. However, NBFA applies a single-layer linear combination of the latent representations, i.e.,  $\sum_k^K \phi_{vk} \theta_{kj}$ , which limits its capacity of capturing cross-excitation. While NBVAE can be viewed as a deep extension of NBFA, using a deep neural network to conduct multi-layer nonlinear combinations of the latent representations, i.e.,  $r_{v,j} = \exp(f_{\theta^r}(\mathbf{z}_j))_v$  and  $p_{v,j} = 1/(1 + \exp(-f_{\theta^p}(\mathbf{z}_j)))_v$ . Therefore, NBVAE en-

Table 3: How different models capture self- and cross-excitation

Model	Self-excitation	Cross-excitation
PFA	Single-layer structure	
LDA	Single-layer structure	
MultiVAE	Multi-layer neural networks	
NBFA	$y_{vj}^{-i}$	Single-layer structure
NBVAE/NBVAE <sub>dm</sub>	$y_{vj}^{-i}$	Multi-layer neural networks

joys richer modelling capacity than NBFA, which is expected to better capture cross-excitation. **3)** Although building multi-layer Bayesian priors is an alternative way to increase the modelling capacity of PFA, LDA, and NBFA, such as further factorising  $\theta$  Gan et al. (2015b); Henao et al. (2015); Zhou et al. (2016) and/or  $\phi$  Zhao et al. (2018), a major advantage of using the VAE framework in our models is that the amortized variational inference is usually more scalable and flexible than conventional Bayesian inference such as Markov chain Monte Carlo (MCMC). As we are dealing with large-scale discrete data, this advantage is especially critical. Finally, we summarise our comparisons of how self- and cross-excitation are captured in related models in Table 3.

### 2.3 NBVAE for Binary Matrices

In many problems, the discrete observations are binary-valued. Simply treating them as counts like in MultiVAE Krishnan et al. (2018); Liang et al. (2018) can result in inferior performance. In contrast, NBVAE generates a sample’s attributes individually from the negative-binomial distributions, instead of jointly generating them from the multinomial distribution. This enables us to develop a simple yet effective method that links NBVAE and the Bernoulli distribution for binary data<sup>4</sup>.

To extend the proposed NBVAE so that it can deal with a binary matrix  $\mathbf{Y} \in \{0, 1\}^{V \times N}$ , we make use of the idea of the link function introduced in Zhou (2015). We first draw a  $V$  dimensional vector of random counts from NBVAE and then generate binary attributes of a sample by thresholding the counts at one, detailed as follows:

$$\mathbf{m}_j \sim \text{NBVAE}(\mathbf{z}_j), \quad (14)$$

$$\mathbf{y}_j = \mathbf{1}(\mathbf{m}_j \geq 1), \quad (15)$$

where “NBVAE” stands for the generative process of NBVAE given  $\mathbf{z}_j$ ,  $\mathbf{m}_j \in \mathbb{N}^V$ , and  $\mathbf{1}(\cdot)$  is the indicator function.  $m_{vj}$  in  $\mathbf{m}_j$  is the latent discrete intensity of

<sup>4</sup>Note that NBVAE<sub>dm</sub> cannot be extended to binary data because the attributes are jointly generated from the Dirichlet-multinomial distribution.

attribute  $v$  being ON in sample  $j$ . As  $\mathbf{m}_j$  is drawn from negative-binomial, we do not have to explicitly generate it. Instead, if we marginalise it out, we can get the following data likelihood:

$$\mathbf{y}_j \sim \text{Bernoulli} \left( 1 - (1 - \mathbf{p}_j)^{\mathbf{r}_j} \right), \quad (16)$$

where  $\mathbf{r}_j$  and  $\mathbf{p}_j$  have the same construction of the original NBVAE. For convenience, we refer this extension of NBVAE as to NBVAE<sub>b</sub> (b for binary).

## 3 Variational Inference

In this section, we give the details on how to learn the proposed NBVAE, NBVAE<sub>dm</sub>, and NBVAE<sub>b</sub> with variational inference. Following the standard amortized variational inference procedure of VAEs, instead of directly deriving the posterior of a model  $p(\mathbf{z}_j | \mathbf{y}_j)$ , we propose a data-dependent variational distribution  $q(\mathbf{z}_j | \mathbf{y}_j)$  to approximate the true posterior, constructed as follows:

$$\tilde{\boldsymbol{\mu}}_j, \tilde{\boldsymbol{\sigma}}_j^2 = f_\phi(\mathbf{y}_j), \quad (17)$$

$$\mathbf{z}_j \sim \mathcal{N}(\tilde{\boldsymbol{\mu}}_j, \text{diag}\{\tilde{\boldsymbol{\sigma}}_j^2\}) \quad (18)$$

As the variational distribution transforms a sample’s attributes into its latent representation, it is referred as to the encoder of VAEs.

Given  $q(\mathbf{z}_j | \mathbf{y}_j)$ , the learning objective is to maximise the Evidence Lower BOund (ELBO) of the marginal likelihood of the data, in terms of the decoder parameters  $\theta^r$ ,  $\theta^p$  and the encoder parameter  $\phi$ . The ELBO of the  $j^{\text{th}}$  sample can be formulated as follows:

$$\mathbb{E}_{q(\mathbf{z}_j | \mathbf{y}_j)} [\log p(\mathbf{y}_j | \mathbf{z}_j)] - \text{KL} [q(\mathbf{z}_j | \mathbf{y}_j) \| p(\mathbf{z}_j)] \quad (19)$$

where  $p(\mathbf{y}_j | \mathbf{z}_j)$  corresponds to Eq. (5), Eq. (10), and Eq. (16) for NBVAE, NBVAE<sub>dm</sub>, and NBVAE<sub>b</sub>, respectively.

To estimate the expectation term on the left-hand side of the ELBO, we need to do sampling from  $q(\mathbf{z}_j | \mathbf{y}_j)$ , making it nontrivial to take gradients with respect to  $\phi$ . Using the reparametrization trick Kingma and Welling (2013); Rezende et al. (2014), we are able to sidestep this problem by:  $\boldsymbol{\epsilon} \sim \mathcal{N}(\mathbf{0}, \mathbf{I}_K)$  and reparametrize  $\mathbf{z}_j := \tilde{\boldsymbol{\mu}}_j + \boldsymbol{\epsilon} \odot \tilde{\boldsymbol{\sigma}}_j^2$ . The Kullback-Leiber (KL) divergence on the right-hand side of the ELBO is calculated between the variational distribution and the prior distribution. The inference algorithm is shown in Algorithm 1.

## 4 Related Work

In this section, we review the existing methods that are closely related to ours. This can be categorised into two main categories as follows.

---

**Algorithm 1** The learning algorithm of NBVAE, NBVAE<sub>dm</sub>, and NBVAE<sub>b</sub>.

---

```

1: Inputs: Discrete matrix  $\mathbf{Y}$ 
2: Randomly initialise  $\theta^r, \theta^p, \phi$ 
3: while not converged do
4:   Sample a batch of samples  $\mathcal{B}$ 
5:   for all  $\mathbf{x}_j \in \mathcal{B}$  do
6:     Sample  $\mathbf{z}_j \sim q(\mathbf{z}_j | \mathbf{y}_j)$ 
7:     Compute the gradients of EBLO with respect
       to  $\theta^r, \theta^p, \phi$ 
8:   end for
9:   Update  $\theta^r, \theta^p, \phi$ 
10: end while
11: Outputs:  $\theta^r, \theta^p, \phi$ 

```

---

**Probabilistic matrix factorisation models for discrete data.** Lots of well-known models fall into this category, including Latent Dirichlet Allocation Blei et al. (2003) and Poisson Factor Analysis Zhou et al. (2012), as well as their hierarchical extensions such as Hierarchical Dirichlet Process Teh et al. (2012), nested Chinese Restaurant Process (nCRP) Blei et al. (2010), nested Hierarchical Dirichlet Process (nHDP) Paisley et al. (2015), Deep Poisson Factor Analysis (DPFA) (Gan et al., 2015a), Deep Exponential Families (DEF) (Ranganath et al., 2015), Deep Poisson Factor Modelling (DPFM) (Henao et al., 2015), and Gamma Belief Networks (GBNs) (Zhou et al., 2016). Among various models, the closest ones to ours are Negative Binomial Factor Analysis (NBFA) Zhou (2018), which uses the negative binomial distribution to model self-excitation of count-valued data, and non-parametric LDA (NP-LDA) Buntine and Mishra (2014) which uses a Dirichlet-multinomial. Our model can be viewed as a deep generative extension of NBFA, providing a more powerful expressive capacity and flexibility than NBFA, which is with a flat structure. In terms of inference, MCMC is used by most of the aforementioned models, which may suffer from scalability issues in both the training and testing phases (averaging over multiple samples is however desired to make predictions). Whereas the inference of our proposed VAE-based models is done by AVI, which enjoys not only excellent scalability but also better flexibility and usability for large-scale data.

**VAEs for discrete data.** Compared to the extensive applications in image analysis, VAEs for discrete data are relatively rare. Miao et al. (2016) proposed the Neural Variational Document Model (NVDM), which extended the standard VAE with multinomial likelihood for document modelling and Miao et al. (2017) further built a VAE to generate the document-topic

distributions in the LDA framework. Srivastava and Sutton (2017) developed an AVI algorithm for the inference of LDA, which can be viewed as a VAE model, although the generative process is the same as the original LDA. Card et al. (2018) introduced a general VAE framework for topic modelling, which is able to incorporate meta-data. Grønbech et al. (2019) recently proposed a Gaussian mixture VAE with negative-binomial for gene data, which has a different construction to ours and the paper does not consider DirMulti or binary construction, or in-depth analysis. Krishnan et al. (2018) recently found that using the standard training algorithm of VAEs in large sparse discrete data may suffer from model underfitting and they proposed Non-linear Factor Analysis (NFA) with a stochastic variational inference (SVI) Hoffman et al. (2013) algorithm initialised by AVI to mitigate this issue. In the collaborative filtering domain, Liang et al. (2018) noticed a similar issue and alleviated it by proposing MultiVAE with a training scheme based on KL annealing Bowman et al. (2016). Note that NVDM, NFA, and MultiVAE are the closest ones to ours, the generative processes of the three models are very similar but their inference procedures are different. NFA is reported to outperform NVDM on text analysis Krishnan et al. (2018) while MultiVAE is reported to have better performance than NFA on collaborative filtering tasks Liang et al. (2018). Although our models are targeted on sparse discrete data as well, we improve the modelling performance in a different way, i.e., by better capturing self- and cross-excitation so as to better handle overdispersion. Moreover, NFA and MultiVAE work with the multinomial distribution, which may not work properly for binary data. Whereas our proposed NBVAE<sub>b</sub> models binary data with the Bernoulli distribution.

## 5 Experiments

In this section, we evaluate the proposed models on two important applications of discrete data: text analysis and collaborative filtering. These experiments are conducted on large-scale real-world datasets including both count-valued and binary ones, demonstrating that our models achieve the state-of-the-art performances on the two tasks compared with several most recent advances.

### 5.1 Experiments on Text Analysis

Our first set of experiments is on text analysis.

Table 4: Statistics of the datasets. The number of nonzeros and density are computed of each whole dataset.

Dataset	$N_{\text{train}}$	$N_{\text{test}}$	V	#Nonzeros	Density
20NG	11,315	7,531	2,000	774,984	0.0343
RCV	794,414	10,000	10,000	58,637,816	0.0074
Wiki	10,000,000	1,000	7,702	82,311,745	0.0107
ML-10M	49,167	10,000	10,066	4,131,372	0.0059
ML-20M	116,677	10,000	20,108	9,128,733	0.0033
Netflix	383,435	40,000	17,769	50,980,816	0.0062
MSD	459,330	50,000	36,716	29,138,887	0.0014

### 5.1.1 Datasets

We used three widely-used corpora Srivastava et al. (2013); Gan et al. (2015a); Henao et al. (2015); Cong et al. (2017): 20 News Group (20NG), Reuters Corpus Volume (RCV), and Wikipedia (Wiki). The details of these datasets are shown in Table 4. The first two datasets were downloaded from the code repository of Gan et al. (2015a)<sup>5</sup>. The Wiki dataset was downloaded from *Wikipedia* using the scripts provided in Hoffman et al. (2010).

### 5.1.2 Metric

We report per-heldout-word perplexity of all the models, which is a widely-used metric for text analysis. Following the approach in Wallach et al. (2009), after training a model with the training documents, we randomly selected some words as the observed words and used the remaining words as the unobserved words in each testing document, then used the observed words to estimate the predictive probability, and finally computed the perplexity of the unobserved words. Specifically, suppose that the matrix of the testing documents is  $\mathbf{Y}^* \in \mathbb{N}^{V \times N_{\text{test}}}$ , which is split into the observed word matrix  $\mathbf{Y}^{*\text{o}} \in \mathbb{N}^{V \times N_{\text{test}}}$  and the unobserved word matrix  $\mathbf{Y}^{*\text{u}} \in \mathbb{N}^{V \times N_{\text{test}}}$ , where  $\mathbf{Y}^* = \mathbf{Y}^{*\text{o}} + \mathbf{Y}^{*\text{u}}$ . The predictive distributions of the testing documents are estimated with  $\mathbf{Y}^{*\text{o}}$  and used to compute the perplexity of  $\mathbf{Y}^{*\text{u}}$ , detailed as follows<sup>6</sup>:

$$\text{Perplexity} = \exp - \left( \frac{1}{y_{..}^{*\text{u}}} \sum_j^{N_{\text{test}}} \sum_v^V y_{vj}^{*\text{u}} \log \frac{l_{vj}}{l_{..j}} \right) \quad (20)$$

where  $y_{..}^{*\text{u}} = \sum_j^{N_{\text{test}}} \sum_v^V y_{vj}^{*\text{u}}$ . Note that the derivation of  $l_{vj}$  is model specific, which is shown in Table 2. To

<sup>5</sup>[https://github.com/zhegan27/dpfa\\_icml2015](https://github.com/zhegan27/dpfa_icml2015)

<sup>6</sup>Our perplexity calculation is the same with the ones in Gan et al. (2015a); Henao et al. (2015); Cong et al. (2017), but different from the ones in Miao et al. (2017, 2016); Krishnan et al. (2018), which use ELBO obtained from all the words of a testing document without splitting it. The results of Miao et al. (2017, 2016); Krishnan et al. (2018) can only be compared with models with variational inference.

conduct a fair comparison of perplexity, the settings of the datasets including the preprocessing process, the training/testing splits, the observed/unobserved words splits, and the perplexity calculation are consistent with those in Gan et al. (2015a); Henao et al. (2015); Cong et al. (2017).

### 5.1.3 Baselines

We compared our proposed NBVAE and NBVAE<sub>dm</sub> with the following three categories of state-of-the-art models for text analysis: **1)** Bayesian deep extensions of PFA and LDA: DLDA Cong et al. (2017), DPFM (Henao et al., 2015), DPFA Gan et al. (2015b) with different kinds of inference algorithms such as Gibbs sampling, stochastic variational inference, and stochastic gradient MCMC (SGM-CMC) Chen et al. (2014); **2)** NBFA Zhou (2018), is a recently-proposed single-layer factor analysis model with negative-binomial likelihood, whose inference is done by Gibbs sampling. As NBFA is a nonparametric model, we used its truncated version to compare with other models. **3)** MultiVAE Liang et al. (2018); Krishnan et al. (2018), a recent VAE model for discrete data with the multinomial distribution as the data distribution. We used the implementation of MultiVAE in Liang et al. (2018).

### 5.1.4 Experimental Setup

In terms of model settings of our proposed models, following Liang et al. (2018), we used the same settings as for MultiVAE. Specifically, we applied the multi-layer perceptrons (MLP) with tanh as the nonlinear activation function between the layers of the encoder and the decoder. We used the same network architecture for  $f_{\theta^r}(\cdot)$  and  $f_{\theta^p}(\cdot)$  (only applicable to NBVAE) and the architecture of  $f_{\phi}(\cdot)$  is symmetric to those of  $f_{\theta^r}(\cdot)$  and  $f_{\theta^p}(\cdot)$ . Moreover, the output layers of  $f_{\theta^r}(\cdot)$ ,  $f_{\theta^p}(\cdot)$ ,  $f_{\phi}(\cdot)$  have no activation function. We set the batch size to 500 and 2000 for 20NG and the other two larger datasets, respectively. The number of training epochs was set to 300. The optimisation of the VAE models was done by Adam Kingma and Ba (2014) with 0.003 as the learning rate. For the baselines, we used the original model settings provided in the code published by the authors. For the VAE-based models, we report the perplexity computed with the parameters (the encoder and decoder) in the last iteration of the training phrase, whereas for models with MCMC sampling (e.g., NBFA), we report the perplexity averaged over multiple samples in the collection iterations.

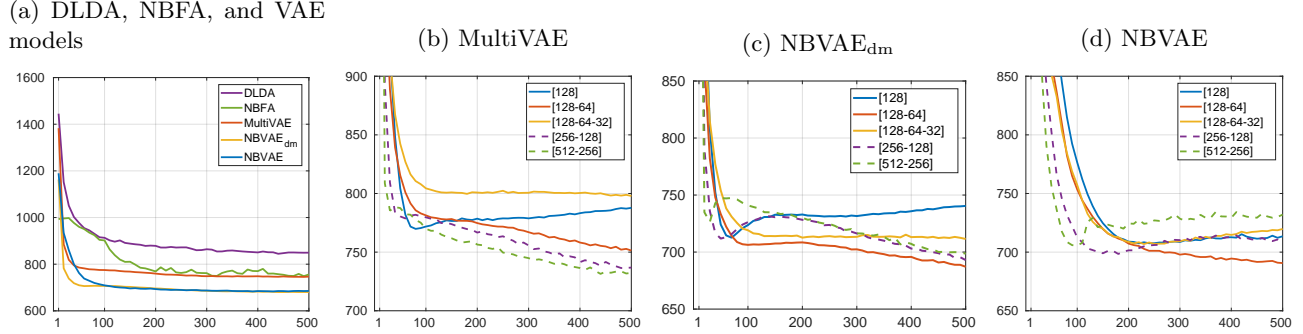


Figure 1: Perplexity of the testing documents over training iterations on the 20NG dataset. (a) Perplexity of DLDA ([128-64-32]), NBVAE ([128]), and VAE models ([128-64]). Unlike in Table 5, where we report the averaged perplexity for DLDA and NBFA, here we report their point perplexity with a single sample, which is expected to be higher than the averaged perplexity. (b)-(d) Perplexity of MultiVAE, NBVAE<sub>dm</sub>, and NBVAE, respectively. Here we varied the depth of the layers and the length of each layer.

Table 5: Perplexity comparisons. Best results for each dataset are in boldface. TLASGR and SGNHT are the algorithms of SGMCMC, detailed in the papers of DLDA Cong et al. (2017) and DPFA Gan et al. (2015a). Some of the results of models with Gibbs sampling on RCV and Wiki are not reported because of the scalability issue.

Model	Inference	Layers	20NG	RCV	Wiki
DLDA	TLASGR	128-64-32	757	815	786
DLDA	Gibbs	128-64-32	752	802	-
DPFM	SVI	128-64	818	961	791
DPFM	MCMC	128-64	780	908	783
DPFA-SBN	Gibbs	128-64-32	827	-	-
DPFA-SBN	SGNHT	128-64-32	846	1143	876
DPFA-RBM	SGNHT	128-64-32	896	920	942
NBFA	Gibbs	128	690	702	-
MultiVAE	VAE	128-64	746	632	629
MultiVAE	VAE	128	772	786	756
NBVAE <sub>dm</sub>	VAE	128-64	<b>680</b>	590	475
NBVAE <sub>dm</sub>	VAE	128	749	709	526
NBVAE	VAE	128-64	685	<b>579</b>	<b>464</b>
NBVAE	VAE	128	714	694	529

Table 6: Perplexity comparisons with larger layer width.

Model	Inference	Layers	RCV	Wiki
DLDA	TLASGR	256-128-64	710	682
NBFA	Gibbs	256	649	-
MultiVAE	VAE	256-128	587	589
NBVAE <sub>dm</sub>	VAE	256-128	552	462
NBVAE	VAE	256-128	535	451
DLDA	TLASGR	512-256-128	656	602
MultiVAE	VAE	512-256	552	558
NBVAE <sub>dm</sub>	VAE	512-256	517	451
NBVAE	VAE	512-256	512	445

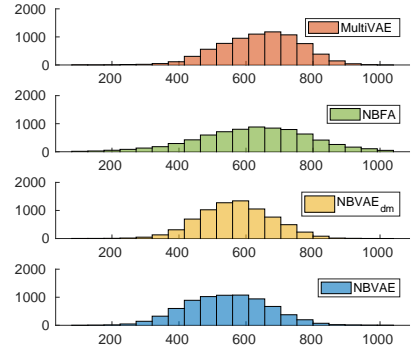


Figure 2: Comparisons of the entropy histograms on the 20NG dataset.

### 5.1.5 Results and Analysis

The perplexity results are shown in Table 5. In this experiment, following the settings of Gan et al. (2015a); Henao et al. (2015); Cong et al. (2017), we report the performance of DLDA, DPFM, and DPFA with two and/or three hidden layers, which are the best results reported in their papers. For the VAE-based models, we varied the network architecture with one and two hidden layers and vary the depth of the layers and the size of each layer later.

Given the perplexity comparisons shown in Table 5, we have the following remarks on the results: **1)** If we compare NBFA with the deep Bayesian models with Poisson distributions listed above it in the table, the results show that modelling self-excitation with the negative-binomial distribution in NBFA has a large contribution to the modelling performance. **2)** It can be observed that the single-layer VAE models (i.e., MultiVAEs with one layer) achieve no better results than NBFA. However, when multi-layer structures were

used, VAE models largely improve their performance. This shows the increased model capacity with deeper neural networks is critical to getting better modelling performance via cross-excitation. **3)** Most importantly, our proposed NBVAE and NBVAE<sub>dm</sub> significantly outperform all the other models, which proves the necessity of modelling self-excitation explicitly and modelling cross-excitation with the deep structures of VAE. **4)** Furthermore, the differences of perplexity between NBVAE and NBVAE<sub>dm</sub> are quite marginal, which is in line with the fact that they are virtually equivalent representations of the same model.

To study why our models achieve better perplexity results than the others, we conducted an additional set of experiments with an in-depth analysis as follows.

**Perplexity with larger layer width.** In Table 5, we followed the settings of Gan et al. (2015a); Henao et al. (2015); Cong et al. (2017) to set up the network structure, where 128 was used as the maximum layer width. Given the sizes of RCV and Wiki, we increased the maximum to 256 and 512 to further compare the results of related models and study if the width of layer matters in the modelling. The results are shown in Table 6. If jointly looking at Table 5 and Table 6, we find **1)** with the increased layer widths, all the models have gained significant improvement. **2)** Among all the models, regardless of the number of neurons used in each layer, both NBVAE and NBVAE<sub>dm</sub> outperform the others with a significant margin. **3)** the table also shows that with smaller model structures (i.e., [256-128]), NBVAE and NBVAE<sub>dm</sub> is able to achieve comparable results with the other models with larger structures, further demonstrating our model’s expressiveness.

**Comparisons of convergence speed.** Here we compare the perplexity convergence speed of our models with DLDA, NBFA, and MultiVAE, in Figure 1a. It can be seen that VAE models enjoys faster convergence speed than DLDA and NBFA using MCMC sampling. Moreover, to estimate the posterior of DLDA and NBFA, we need to average over multiple samples. To do so, the algorithm needs to iterate over the testing documents multiple times. Whereas our models are able to derive good results with a single sample. Furthermore, although NBVAE and NBVAE<sub>dm</sub> achieve similar results after their convergence, NBVAE<sub>dm</sub> converges slightly faster, as NBVAE<sub>dm</sub> has fewer parameters than NBVAE.

**Overfitting/Underfitting of VAE models.** Unlike conventional Bayesian models with hierarchical prior distributions such as DLDA, it is known that VAE models are sensitive to the dimensions of the latent representations and the encoder/decoder struc-

tures. Here we study how the performance of the VAE models on 20NG varies with different settings, shown in Figure 1b to 1d. It can be seen that increasing the layer widths from [128-64] to [256-128] and [512-256] improves MultiVAE’s performance but it is not the case for NBVAE and NBVAE<sub>dm</sub>. This is because that NBVAE and NBVAE<sub>dm</sub> have more parameters than MultiVAE, so increasing the parameter space will cause overfitting in the two models more easily. As NBVAE is with more parameters than NBVAE<sub>dm</sub>, the overfitting in NBVAE is more obvious<sup>7</sup>. Now we compare the cases where the encoder/decoder structures go from [128] to [128-64] and [128-64-32]. We can observe a similar trend in the three models, i.e., [128-64] performs the best and going deeper or shallower gets inferior performance. Using the settings of [128] means that we have a large dimension of the latent representations but the encoder/decoder networks are quite shallow, which may not be able to learn good representations. On the contrary, with [128-64-32], although the networks are deep, the dimensions of the latent representations may be too small to learn a good model. This set of experiments demonstrate that model selection is important to the VAE models that we are comparing with, but studying the details is outside the paper and we leave it for future study.

**Comparisons of predictive distribution entropy.** To further analyse the predictive distributions of related models, we compare the entropy of the predictive distributions on the testing documents of 20NG. The entropy of document  $j$  given the predictive distribution parameterised with  $\mathbf{l}'_j$  is computed as follows:

$$\text{entropy}_j = \exp \left( - \sum_v^V l'_{vj} \log(l'_{vj}) \right), \quad (21)$$

where  $\mathbf{l}'_j$  is assumed to be normalised and is computed model-specifically according to Table 2.

After computing the entropy of all the testing documents, we plot the histograms in Figure 2. The intuition here is that the entropy of the predictive distribution of a document can be viewed as the effective number of unique words that the document is expected to focus on, given a model. Therefore, if a model takes self-excitation into account, the entropy of a document is expected to be small, because the model’s predictive distribution will put large mass on the words that already occur in the document. That is to say, the document is expected to focus on the existing words. Whereas if a model without the consideration of self-excitation, its predictive distribution of

<sup>7</sup>Note that compared with RCV and Wiki, 20NG is a relatively small dataset. Therefore, unlike results in Table 6, using larger layer widths is easier to cause overfitting.

a document would relatively spread over all the words. Figure 2 shows that the average entropy of our models is smaller than that of MultiVAE, demonstrating the effect of modelling self-excitation.

## 5.2 Experiments on Collaborative Filtering

Our second set of experiments is targeted at collaborative filtering, where the task is to recommend items to users using their clicking history.

### 5.2.1 Datasets

We evaluate our models’ performance on four user-item consumption datasets: MovieLens-10M (ML-10M)<sup>8</sup>, MovieLens-20M (ML-20M)<sup>8</sup>, Netflix Prize (Netflix)<sup>9</sup>, and Million Song Dataset (MSD)<sup>10</sup> Bertin-Mahieux et al. (2011). All the datasets were preprocessed and binarised by the Python code provided by Liang et al. (2018), using the same settings described in the paper. The statistics of the datasets are shown in Table 4. Note that following Liang et al. (2018), we also generated a validation set with the same size of the testing set.

### 5.2.2 Metrics

Two ranking-based metrics were used. They are Recall@ $R$  and the truncated normalized discounted cumulative gain (NDCG@ $R$ ). To compute those metrics, following Liang et al. (2018), we first estimated the parameters  $\mathbf{l}'_j$  of the predictive distribution of user  $j$  given the observed items  $\mathbf{y}_j^{*o}$ , and then ranked the unobserved items  $\mathbf{y}_j^{*u}$  by sorting  $\mathbf{l}'_j$ . The metrics are computed as follows:

$$\text{Recall}@R = \frac{\sum_{r=1}^R \mathbf{1}(y_{\omega(r),j}^{*u} = 1)}{\min(R, y_j^{*u})} \quad (22)$$

$$\text{DCG}@R = \frac{\sum_{r=1}^R 2^{\mathbf{1}(y_{\omega(r),j}^{*u} = 1)} - 1}{\log(r+1)} \quad (23)$$

where  $\omega(r) \in \{1, \dots, V\}$  is the item at rank  $r$ , which is obtained by sorting the predictive probability of the user;  $\mathbf{1}(y_{\omega(r),j}^{*u} = 1)$  indicates whether the item is actually clicked on by user  $j$ ; NDCG@ $R$  is computed by linearly normalising DCG@ $R$  into  $[0, 1]$ . Intuitively, Recall@ $R$  measures the number of the  $R$  predicted items that are within the set of the ground-truth items but does not consider the item rank in  $R$ , while NDCG@ $R$  assigns larger discounts to lower

<sup>8</sup><https://grouplens.org/datasets/movielens/>

<sup>9</sup><http://www.netflixprize.com/>

<sup>10</sup><https://labrosa.ee.columbia.edu/millionsong/>

ranked items. In the experiments, we used the code provided in Liang et al. (2018) to compute the above two metrics. Moreover, we report the testing performance of the models with the best NDCG@50 on the validation set.

### 5.2.3 Baselines

Recall that datasets used here are binary. So we compared NBVAE<sub>b</sub>, with the following two recent VAE models: **1**) MultiVAE. **2**) MultiDAE Liang et al. (2018), a denoising autoencoder (DAE) with multinomial likelihood, which introduces dropout Srivastava et al. (2014) at the input layer. MultiVAE and MultiDAE are the state-of-the-art VAE models for collaborative filtering and they have been reported to outperform several recent advances such as Wu et al. (2016) and He et al. (2017).

### 5.2.4 Experimental Setup

For NBVAE, NBVAE<sub>dm</sub>, and NBVAE<sub>b</sub>, we used the same settings as in the text analysis experiments, except that: **1**) The batch size was set to 500 for all the datasets. **2**) The width of the hidden layers for the decoder and encoder was set to [600-200]. **3**) We used the same KL annealing procedure of MultiVAE and the annealing cap  $\beta$  was set to 0.2. Note that all the above settings are consistent with those in Liang et al. (2018) The original code of MultiVAE and MultiDAE and their default settings provided by the authors were used in the comparison.

### 5.2.5 Results and Analysis

Figure 3 shows the NDCG@ $R$  and Recall@ $R$  of the models on the four datasets, where we used  $R \in \{1, 5, 10, 20, 50\}$ . In general, our proposed NBVAE<sub>b</sub> outperforms the baselines (i.e., MultiVAE and MultiDAE) on almost all the datasets. In particular, the margin is notably large while the  $R$  value is small, such as 1 or 5. It indicates that the top-ranked items in NBVAE<sub>b</sub> are always more accurate than those ranked by MultiVAE and MultiDAE. This fact is also supported by the large gap in terms of NDCG@ $R$  between the performance of NBVAE<sub>b</sub> and the two baselines, as NDCG@ $R$  penalises the true items that are ranked low by the model.

The experimental results show that it is beneficial to model binary data directly with a binary model, instead of treating them as count-valued data with multinomial like in MultiVAE and MultiDAE. To further demonstrate this, we compare NBVAE<sub>b</sub> with NBVAE and NBVAE<sub>dm</sub> on the ML-10M dataset, where the

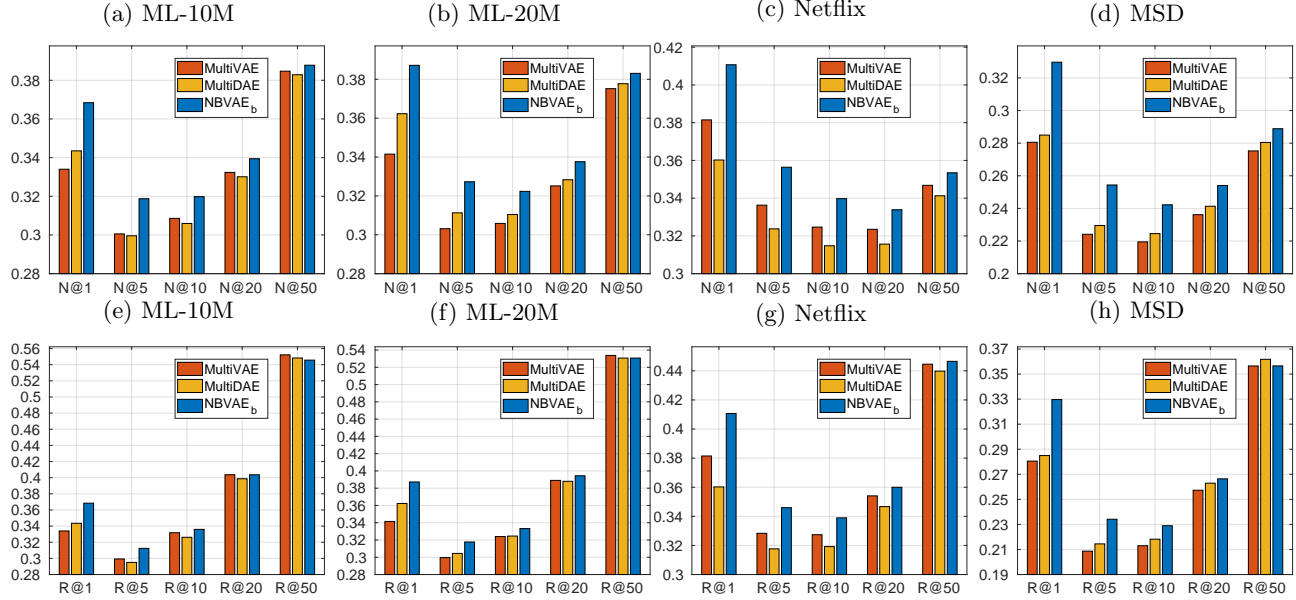


Figure 3: Comparisons of NDCG@R (N@R) and Recall@R (R@R). Standard errors are less than 0.003 for all the models on all the datasets.

Table 7: NDCG@R (N@R) and Recall@R (R@R) of NBVAE and its variants on ML-10M. Best results are in boldface.

Model	N@1	N@5	N@10	N@20	N@50	R@1	R@5	R@10	R@20	R@50
NBVAE	0.3333	0.2951	0.3012	0.3263	0.3788	0.3333	0.2927	0.3224	0.3968	0.5453
NBVAE <sub>dm</sub>	0.3441	0.3034	0.3070	0.3294	0.3800	0.3441	0.3005	0.3270	0.3978	0.5441
<b>NBVAE<sub>b</sub></b>	<b>0.3684</b>	<b>0.3187</b>	<b>0.3198</b>	<b>0.3394</b>	<b>0.3878</b>	<b>0.3684</b>	<b>0.3124</b>	<b>0.3360</b>	<b>0.4039</b>	<b>0.5456</b>

latter two models treat binary data as count-valued data. The results of NDCG@R and Recall@R on ML-10M are shown in Table 7. It can be observed that NBVAE<sub>b</sub>'s results are significantly better than NBVAE and NBVAE<sub>dm</sub>, showing the necessity of dealing with binary data separately from count-valued data.

## 6 Conclusion

We focussed on analysing and tackling overdispersion in large-scale discrete data with deep generative models. Specifically, we have given detailed analysis on how related models capture self- and cross-excitation in discrete data, and demonstrated that to better model overdispersion, it is necessary to deal with both kinds of excitations properly. To achieve this, we have proposed a VAE framework using negative-binomial as the data distribution, where the mechanism of the negative-binomial distribution explicitly captures self-excitation and deep neural networks of VAE framework help model cross-excitation better. In addition, unlike many of the existing models, which may misuse a multinomial for modelling binary data, the proposed NBVAE enables developing a link function between

the negative-binomial and Bernoulli, which is a proper approach working on binary data. To demonstrate our models' advantages, we have conducted extensive experiments on text corpora and collaborative filtering datasets. The proposed NBVAE and NBVAE<sub>dm</sub> achieve the state-of-the-art performance in terms of perplexity on text analysis and our NBVAE<sub>b</sub> outperforms the recent VAE advances in collaborative filtering in terms of ranking-based metrics, Recall@R and NDCG@R, on several benchmark datasets.

## References

Thierry Bertin-Mahieux, Daniel P.W. Ellis, Brian Whitman, and Paul Lamere. 2011. The Million Song Dataset. In *the 12th International Conference on Music Information Retrieval (ISMIR 2011)*.

David M Blei, Thomas L Griffiths, and Michael I Jordan. 2010. The nested Chinese restaurant process and Bayesian nonparametric inference of topic hierarchies. *Journal of the ACM (JACM)* 57, 2 (2010), 7.

David M Blei, Andrew Y Ng, and Michael I Jordan.

2003. Latent Dirichlet allocation. *JMLR* 3 (2003), 993–1022.

Samuel R Bowman, Luke Vilnis, Oriol Vinyals, Andrew Dai, Rafal Jozefowicz, and Samy Bengio. 2016. Generating sentences from a continuous space. In *CoNLL*. 10–21.

Wray L Buntine and Swapnil Mishra. 2014. Experiments with non-parametric topic models. In *SIGKDD*. 881–890.

John Canny. 2004. GaP: a factor model for discrete data. In *SIGIR*. 122–129.

Dallas Card, Chenhao Tan, and Noah A Smith. 2018. Neural models for documents with metadata. In *ACL*. 2031–2040.

Tianqi Chen, Emily Fox, and Carlos Guestrin. 2014. Stochastic gradient Hamiltonian Monte Carlo. In *ICML*. 1683–1691.

Kenneth W Church and William A Gale. 1995. Poisson mixtures. *Natural Language Engineering* 1, 2 (1995), 163–190.

Yulai Cong, Bo Chen, Hongwei Liu, and Mingyuan Zhou. 2017. Deep latent Dirichlet allocation with topic-layer-adaptive stochastic gradient Riemannian MCMC. In *ICML*. 864–873.

Gabriel Doyle and Charles Elkan. 2009. Accounting for burstiness in topic models. In *ICML*. 281–288.

Zhe Gan, Changyou Chen, Ricardo Henao, David Carlson, and Lawrence Carin. 2015a. Scalable deep Poisson factor analysis for topic modeling. In *ICML*. 1823–1832.

Zhe Gan, R. Henao, D. Carlson, and Lawrence Carin. 2015b. Learning deep sigmoid belief networks with data augmentation. In *AISTATS*. 268–276.

Olivier Gouvert, Thomas Oberlin, and Cédric Févotte. 2018. Negative binomial matrix factorization for recommender systems. *arXiv preprint arXiv:1801.01708* (2018).

Christopher Heje Grønbech, Maximillian Fornitz Vording, Pascal Nordgren Timshel, Casper Kaae Sønderby, Tune Hannes Pers, and Ole Winther. 2019. scVAE: Variational auto-encoders for single-cell gene expression data. *bioRxiv* (2019), 318295.

Xiangnan He, Lizi Liao, Hanwang Zhang, Liqiang Nie, Xia Hu, and Tat-Seng Chua. 2017. Neural collaborative filtering. In *WWW*. 173–182.

Ricardo Henao, Zhe Gan, James Lu, and Lawrence Carin. 2015. Deep Poisson factor modeling. In *NIPS*. 2800–2808.

Matthew Hoffman, Francis R Bach, and David M Blei. 2010. Online learning for latent Dirichlet allocation. In *NIPS*. 856–864.

Matthew D Hoffman, David M Blei, Chong Wang, and John Paisley. 2013. Stochastic variational inference. *JMLR* 14, 1 (2013), 1303–1347.

Diederik P Kingma and Jimmy Ba. 2014. Adam: A method for stochastic optimization. *arXiv preprint arXiv:1412.6980* (2014).

Diederik P Kingma and Max Welling. 2013. Auto-encoding variational Bayes. *arXiv preprint arXiv:1312.6114* (2013).

Rahul Krishnan, Dawen Liang, and Matthew Hoffman. 2018. On the challenges of learning with inference networks on sparse, high-dimensional data. In *AISTATS*. 143–151.

Dawen Liang, Rahul G Krishnan, Matthew D Hoffman, and Tony Jebara. 2018. Variational autoencoders for collaborative filtering. In *WWW*. 689–698.

Rasmus E Madsen, David Kauchak, and Charles Elkan. 2005. Modeling word burstiness using the Dirichlet distribution. In *ICML*. 545–552.

Yishu Miao, Edward Grefenstette, and Phil Blunsom. 2017. Discovering discrete latent topics with neural variational inference. In *ICML*. 2410–2419.

Yishu Miao, Lei Yu, and Phil Blunsom. 2016. Neural variational inference for text processing. In *ICML*. 1727–1736.

Andriy Mnih and Ruslan R Salakhutdinov. 2008. Probabilistic matrix factorization. In *NIPS*. 1257–1264.

John Paisley, Chong Wang, David M Blei, and Michael I Jordan. 2015. Nested hierarchical Dirichlet processes. *TPAMI* 37, 2 (2015), 256–270.

Rajesh Ranganath, Linpeng Tang, Laurent Charlin, and David Blei. 2015. Deep exponential families. In *AISTATS*. 762–771.

Danilo Jimenez Rezende, Shakir Mohamed, and Daan Wierstra. 2014. Stochastic backpropagation and approximate inference in deep generative models. In *ICML*. 1278–1286.

Akash Srivastava and Charles Sutton. 2017. Autoencoding Variational Inference For Topic Models. (2017).

Nitish Srivastava, Geoffrey Hinton, Alex Krizhevsky, Ilya Sutskever, and Ruslan Salakhutdinov. 2014. Dropout: a simple way to prevent neural networks from overfitting. *JMLR* 15, 1 (2014), 1929–1958.

Nitish Srivastava, Ruslan Salakhutdinov, and Geoffrey Hinton. 2013. Modeling documents with a Deep Boltzmann Machine. In *UAI*. 616–624.

Y.W. Teh, M.I. Jordan, M.J. Beal, and D.M. Blei. 2012. Hierarchical Dirichlet processes. *J. Amer. Statist. Assoc.* 101, 476 (2012), 1566–1581.

H.M. Wallach, I. Murray, R. Salakhutdinov, and D. Mimno. 2009. Evaluation methods for topic models. In *ICML*, L. Bottou and M. Littman (Eds.).

Yao Wu, Christopher DuBois, Alice X Zheng, and Martin Ester. 2016. Collaborative denoising auto-encoders for top-n recommender systems. In *WSDM*. 153–162.

He Zhao, Lan Du, Wray Buntine, and Mingyuan Zhou. 2018. Dirichlet belief networks for topic structure learning. In *NeurIPS*. 7966–7977.

MingYuan Zhou. 2015. Infinite edge partition models for overlapping community detection and link prediction. In *AISTATS*. 1135–1143.

Mingyuan Zhou. 2018. Nonparametric Bayesian negative binomial factor analysis. *Bayesian Analysis* (2018).

Mingyuan Zhou, Yulai Cong, and Bo Chen. 2016. Augmentable gamma belief networks. *JMLR* 17, 163 (2016), 1–44.

Mingyuan Zhou, Lauren Hannah, David B Dunson, and Lawrence Carin. 2012. Beta-negative binomial process and Poisson factor analysis. In *AISTATS*. 1462–1471.